Mobility saturation in tapered edge bottom contact copper phthalocyanine thin film transistors

James E. Royer
Department of Chemistry and Biochemistry, University of California, San Diego, 9500 Gilman Drive, La Jolla, California 92093

Jeongwon Park
Materials Science and Engineering Program, University of California, San Diego, 9500 Gilman Drive, La Jolla, California 92093

Corneliu Colesniuc
Department of Physics, University of California, San Diego, 9500 Gilman Drive, La Jolla, California 92093

Joon Sung Lee
Materials Science and Engineering Program, University of California, San Diego, 9500 Gilman Drive, La Jolla, California 92093

Thomas Gredig
Department of Physics and Astronomy, California State University Long Beach, 1250 Bellflower Boulevard, Long Beach, California 90840, USA

Sangyeob Lee
Department of Chemistry and Biochemistry, University of California, San Diego, 9500 Gilman Drive, La Jolla, California 92093

Sungho Jin
Materials Science and Engineering Program, University of California, San Diego, 9500 Gilman Drive, La Jolla, California 92093

Ivan K. Schuller
Department of Physics, University of California, San Diego, 9500 Gilman Drive, La Jolla, California 92093

William C. Trogler and Andrew C. Kummel[a)]
Department of Chemistry and Biochemistry, University of California, San Diego, 9500 Gilman Drive, La Jolla, California 92093

(Received 12 March 2010; accepted 28 June 2010; published 27 July 2010)

Copper phthalocyanine (CuPc) thin film transistors were fabricated using a tapered edge bottom contact device geometry, and mobility saturation was observed for devices with CuPc thicknesses of 12 monolayers (MLs) and greater. The mobility saturation is attributed to a significantly decreased contact resistance resulting from a bilayer resist lift-off method, as compared with a single layer resist lift-off method. Threshold voltages are also found to saturate above 12 ML CuPc thicknesses. © *2010 American Vacuum Society.* [DOI: 10.1116/1.3464771]

I. INTRODUCTION

The role of contact effects in organic thin film transistors (OTFTs) has been extensively investigated using current-voltage,[1,2] scanning probe,[3,4] and even chemical sensing techniques.[5] Development of processing techniques which can minimize contact resistance are required for further exploration of OTFTs based on novel materials. Numerous reports have been published on the saturation of field effect mobility in OTFTs when the organic semiconductor (OSC) layer exceeds a critical thickness.[6–8] Such reports are in agreement with the calculations by Horowitz, which showed that at sufficiently high gate voltages the majority of carrier transport occurs within the first few OSC monolayers (MLs) above the gate insulator.[9] Most experimental reports utilize top-contact device structures so that the extracted field effect mobility data will not be influenced by parasitic contact resistances. Muck *et al.* showed peaks in the field effect mobility after completion of the first and second monolayer of dihexyl quaterthiophene (DH4T) followed by a drop to the saturation field effect mobility for increased DH4T layers.[7] The drop in mobility with more than 2 ML DH4T was attributed to increased contact resistance in their bottom contact devices. Gao *et al.* recently reported on top contact copper phthalocyanine (CuPc) OTFTs which exhibit saturation in field effect mobility when the CuPc layer exceeds 6 MLs.[8] Using a tapered electrode bottom contact device geometry, we show that a similar mobility saturation in CuPc OTFTs is possible when the contact resistance is minimized.

[a)]Electronic mail: akummel@ucsd.edu

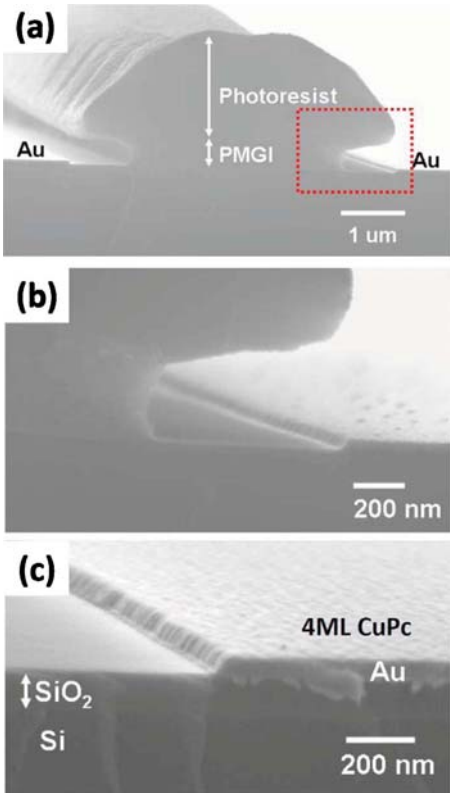

FIG. 1. (Color online) SEM images of bottom contact electrodes from the bilayer process. (a) Metal electrode deposition on the interdigitated pattern using bilayer photoresist photolithography prior to lift-off. (b) High magnification of the dotted area of (a). (c) Cross-section image of a 4ML CuPc layer on the Au electrode after lift-off.

II. EXPERIMENT

A. Electrode fabrication

Substrate-gated, bottom contact OTFTs were fabricated by bilayer photoresist photolithography and lift-off processing[10] on (100) n^+ Si substrates with 100 nm SiO_2, the gate dielectric, from Nova Electronic Materials, Ltd. In the bilayer photoresist lift-off process, two different types of photoresist material with distinct etching rates are utilized; a polymethylglutarimide (PMGI) mixture solution (1:1 ratio of PMGI SF-13 and PMGI SF-3) and Microposit S1818. The PMGI is spin coated first to create about 300 nm high undercut layer and S1818 is spin coated second to create a 2 μm high top resist layer. The underlying PMGI resist layer develops nearly isotropically and etches faster in the Microposit MF319 developer solution (Shipley Corp.) than the top layer S1818. Therefore, the amount of undercut is precisely controlled by the etching rate of PMGI. As shown in Figs. 1(a) and 1(b), a reentrant profile is produced by the differential development rate of the two components of the bilayer resist. Source and drain contacts consisting of 50 Å Ti and 450 Å Au were deposited by electron beam deposition at a rate of 1 Å s^{-1}. The electrodes consist of 45 pairs of gold fingers, with a 5 μm gap and an electrode width of 2 mm. Six pairs of electrodes were grown on each substrate to verify OTFT reproducibility.

B. Thin film deposition

CuPc was deposited by organic molecular beam deposition at room temperature using a rate of ~0.5 Å s^{-1} under high vacuum (base pressure $<1\times10^{-8}$ Torr). CuPc was obtained from Sigma-Aldrich and zone purified at 400 °C and 10^{-5} Torr for over 50 h with a yield over 70%. CuPc films with thicknesses ranging from 4 to 1000 (±5%) MLs were deposited on chips with six OTFT devices per chip to assess reproducibility. Shown in Fig. 1(c) are the cross-sectional scanning electron microscopy (SEM) images of typical electrodes after depositing 4 ML CuPc films, which is the thinnest film in this study. A quartz crystal microbalance (QCM) was used to calculate the CuPc film thickness. The QCM was calibrated with both atomic force microscopy (AFM) and low angle x-ray diffraction (XRD) measurements. XRD measurements were performed using a Rigaku RU-200B diffractometer with Cu $K\alpha$ radiation. XRD revealed the films deposited at 25 °C to be textured α phase. The CuPc molecules in the bulk of the film are oriented perpendicular to the substrate surface with d spacing of 13.3 Å.[11] After deposition, electrical measurements of the devices were recorded within 1 h.

III. RESULTS AND DISCUSSION

The bilayer lift-off process was employed to fabricate the optimal electrode contact geometry for CuPc OTFTs with low contact resistance. 12 ML devices fabricated using the two different electrode geometries were used to show the dependence of contact geometry on the contact resistance. The contact resistance was determined using dc electrical measurements, scanning Kelvin probe microscopy (SKPM), and the transfer line method (TLM). Subsequently, the electrical properties of CuPc OTFTs with tapered contacts were measured as a function of the channel CuPc layer thickness from 4 to 1000 (±5%) MLs. Minimizing the contact resistance ensures that the electrical measurements reflect the intrinsic channel mobility.

A. Optimal CuPc OTFTs with low contact resistance

The current (I)-voltage (V) characteristics were measured with a HP 4155A semiconductor parameter analyzer at 10 V s^{-1} sweep rate in an optically isolated probe station at 25 °C to minimize photocurrent. Figures 2(a) and 2(b) show the representative output characteristics of 12 ML CuPc OTFTs at different gate-source voltages (V_{gs}) from +4 to −12 V for a single layer photoresist lift-off processed device and a bilayer photoresist lift-off processed device.[10] The insets in Fig. 2 show the cross-sectional SEM image and the electrode geometry for each device (note that six devices of each type were fabricated; the data shown in Fig. 2 are representative of all these devices). The output characteristics of the 12 ML CuPc OTFTs using the single layer photoresist lift-off process show a nonlinear behavior at low V_{ds} and no apparent current saturation [Fig. 2(a)], which is consistent with a large contact resistance between the CuPc channel and the source/drain electrodes. Conversely, with the bilayer pho-

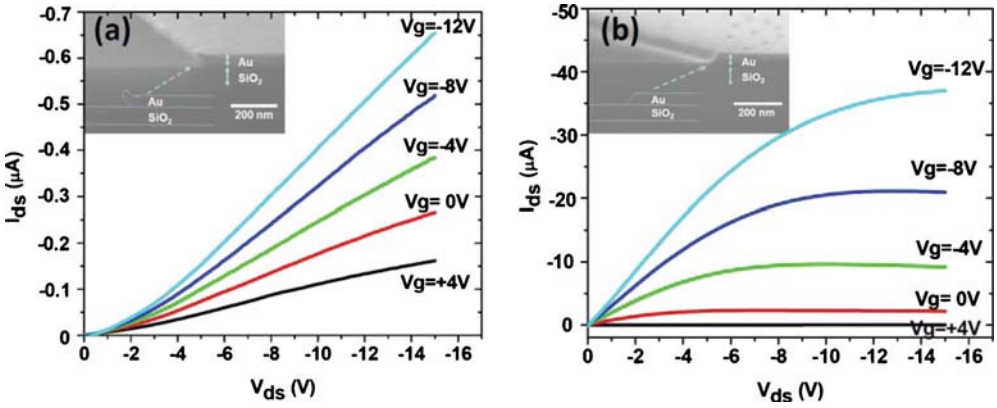

FIG. 2. (Color online) Representative output characteristics of 12 ML CuPc OTFTs with 5 μm channel length. (a) OTFTs with electrodes fabricated with the single layer photoresist and (b) OTFTs with tapered electrodes fabricated with the bilayer photoresist lift-off process. The insets show cross-section SEM images and electrode layouts for each device.

toresist lift-off process, the linear region and the saturation region are clearly observed. Over 100 of the bilayer photoresist lift-off devices of 12 ML thickness were fabricated; all had good saturation behavior at high V_{ds} similar to that shown in Fig. 2(b) consistent with a low contact resistance from the tapered edge shape of the bilayer processed electrodes.[10] To quantify the role of electrode shape, the contact resistances were extracted for single and bilayer processed OTFTs from the linear region of the output curves.[12] The contact resistance values differed by a factor of 2000: at $V_{ds}=-1$ V and $V_{gs}=-12$ V the contact resistances are $1.8\pm2.1\times10^{8}$ and $9.6\pm3.9\times10^{4}$ Ω, respectively, for the single layer and bilayer lift-off processed devices.[10]

To further confirm the low contact resistance in bilayer processed 12 ML CuPc OTFTs, the contact resistance was calculated using the TLM (Ref. 12) from bilayer processed 12 ML OTFTs with channel lengths from 5 to 160 μm (see Fig. 3). In this method, the total resistance is assumed to be the sum of the channel and contact resistances. The TLM contact resistance on bilayer processed 12 ML CuPc OTFTs was 3.7×10^{5} Ω at $V_{gs}=-12$ V, which is comparable to the value obtained from the *I-V* characteristics, considering the differences in drain voltage and channel length between the two methods. To further characterize the role of contact resistance in the poor output characteristics of the single layer processed devices, the surface potentials on the 12 ML single layer and bilayer processed devices were measured by SKPM (Nanoscope IV in tapping mode with a VEECO 200 kHz probe).[13,14] SKPM uses an atomic force microscope tip to map the potential between the source and drain electrodes as a function of gate and source-drain voltages. This allows the contact resistance to be quantified by measuring perturbations to the potential at the source-channel and channel-drain interfaces.[3,15–17] The bilayer photoresist lift-off processed devices have a small symmetric potential drop of 1 V across the source and drain contacts compared to 8 V on the source contact side of the monolayer photoresist lift-off processed devices. The bilayer photoresist lift-off processed device potential drops are sufficiently small that the output characteristics can be employed to calculate the channel mobility accurately.[16] By minimizing the barrier to carrier injection, the bilayer photoresist lift-off process has effectively eliminated contact resistance in the CuPc OTFTs, providing nearly ideal *I-V* characteristics in the linear region as shown in Fig. 2(b).

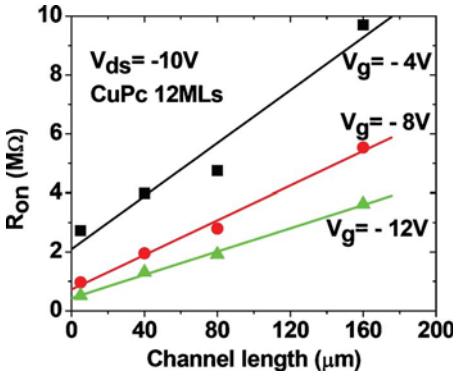

FIG. 3. (Color online) Resistance as a function of channel length from 5 to 160 μm for 12 ML CuPc OTFTs at $V_{ds}=-10$ V and gate voltages (V_{gs}) from -4 to -12 V. The *y*-axis intercepts correspond to the contact resistance of CuPc OTFTs.

B. Thickness effects (AFM, IV)

Figure 4 shows the film morphology of the channel layer with 4–1000 ML CuPc film thickness on devices fabricated with the bilayer photoresist lift-off process. Note that in AFM images, the tops of grains appear as "islands;" in this paper, "grain" and "island" are used interchangeably since the 12–1000 ML films are sufficiently thick that the islands are the tops of the grains instead of the surface topology of a single crystal film. For a 4 ML film thickness, CuPc has a continuous film up to the third layer and contains islands on the top layer of about 21 nm in diameter, as shown in Fig. 4(a). For thicker films, such as 494 ML in Fig. 4(e) and 1000 ML in Fig. 4(f), the growth mechanism competes with various coarsening processes and results in a large island formation.[18] The rms surface roughness increases linearly

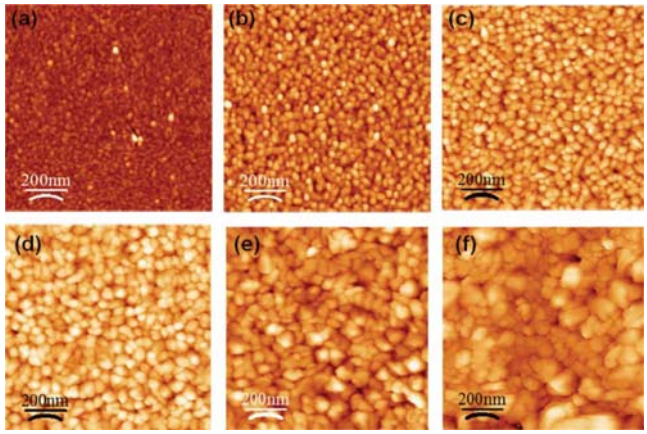

FIG. 4. (Color online) AFM images (1×1 μm) of a CuPc layer on SiO_2 with different CuPc thicknesses. (a) 4, (b) 36, (c) 150, (d) 250, (e) 494, and (f) 1000 ML. rms roughness increases linearly with film thickness at a rate of 0.06 nm/ML. Island size follows a power law of 1/10 with thickness of film.

from 0.7 to 62 nm for the 4 and 1000 ML CuPc films, respectively, but is always a small fraction of the film thickness (Table I).

Among 118 different devices, Fig. 5 shows the representative current-voltage characteristics for CuPc OTFTs with different film thicknesses. In total, 7 (4 ML), 79 (12 ML), 7 (36 ML), 12 (100 ML), 6 (250 ML), and 7 [1000 ($\pm5\%$) ML] devices were fabricated with the bilayer photoresist lift-off process. In order to demonstrate reproducibility, these output characteristics were measured on at least six duplicates for each device, and the output current at saturation at high gate voltages had a standard deviation of less than 33% for all thicknesses. The current-voltage characteristics are similar for devices ranging from 12 to 1000 ML. This is consistent with a charge transport mechanism in which all the carriers conduct in the first few MLs near the gate dielectric.

TABLE I. rms roughness and island size for CuPc films with varying thicknesses.

Thickness (ML)	rms roughness (nm)	Island size (nm)
4	0.74	21
36	4.33	30
150	14.4	35
250	18.8	41
494	29.1	46
1000	62.1	53

In order to examine the consistency of the processing, histograms showing the distributions of on-state currents at $V_g=-12$ V and $V_{ds}=-15$ V for the bilayer lift-off processed OTFTs are displayed in Fig. 6. The histograms show a narrow distribution of device characteristics with different CuPc thicknesses. The relatively narrow distributions of electrical properties in the bilayer lift-off processed devices are consistent with the control of the electrode profile in the first few nanometers above the surface.

The field effect mobilities and threshold voltages can be obtained from the device characteristics in the saturation region $[V_{ds}\geq(V_{gs}-V_{th})]$ based on[19]

$$I_{ds}=\frac{W}{2L}\mu C_i(V_{gs}-V_{th})^2. \quad (1)$$

Here W is the channel width, L is the channel length, C_i is the capacitance per unit area of the insulating layer, V_{th} is the threshold voltage, and μ is the field effect mobility. Figure 6

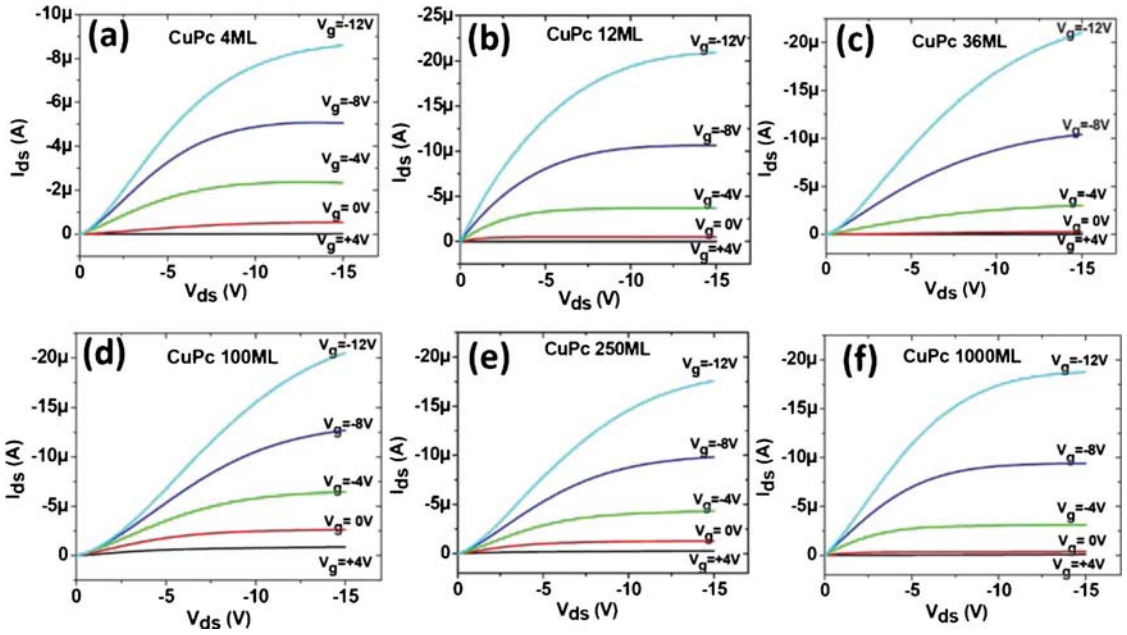

FIG. 5. (Color online) Representative output characteristics of CuPc OTFTs with different CuPc thicknesses. (a) 4, (b) 12, (c) 36, (d) 100, (e) 250, and (f) 1000 ML.

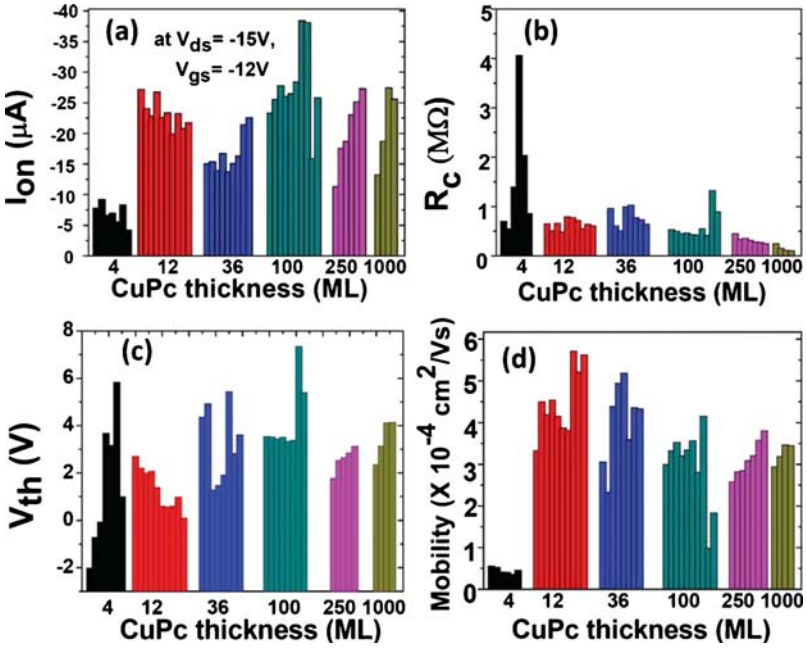

FIG. 6. (Color online) Histograms showing statistical distribution of (a) on-state current at $V_{ds}=-15$ V, $V_g=-12$ V, (b) contact resistance, (c) threshold voltage, and (d) mobility from analysis of 7 (4 ML), 10 (12 ML), 7 (36 ML), 10 (100 ML), 6 (250 ML), and 4 (1000 ML) devices using the bilayer photoresist lift-off process.

shows the variation of the on-current (at $V_{ds}=-10$ V, $V_{gs}=-15$ V), contact resistance, mobility, and threshold voltage for all the devices for each thickness. The variation in on-current is from $(-4.1\pm0.5)\times10^{-6}$ A (4 ML) to $(-34.7\pm5.7)\times10^{-6}$ A (1000 ML). The contact resistance varies from $(2.9\pm2.6)\times10^{6}$ Ω (4 ML) to $(3.1\pm1.3)\times10^{5}$ Ω (1000 ML). The threshold voltage ranges between 2.3 ± 3.3 V (4 ML) and 3.4 ± 0.9 V (1000 ML).

The mean device properties are plotted versus the logarithm of the channel thickness in Fig. 7. The mobility is 4×10^{-4} cm^2 V^1 s^{-1} with a random variation (<2 times) with film thickness except for the 4 ML CuPc OTFTs as shown in Fig. 7(d). The one order of magnitude lower mobility of the 4 ML CuPc devices compared to 12 ML CuPc devices may be due to incomplete film coverage or differences in oxygen doping.[20] A similar dependence on the CuPc thickness was

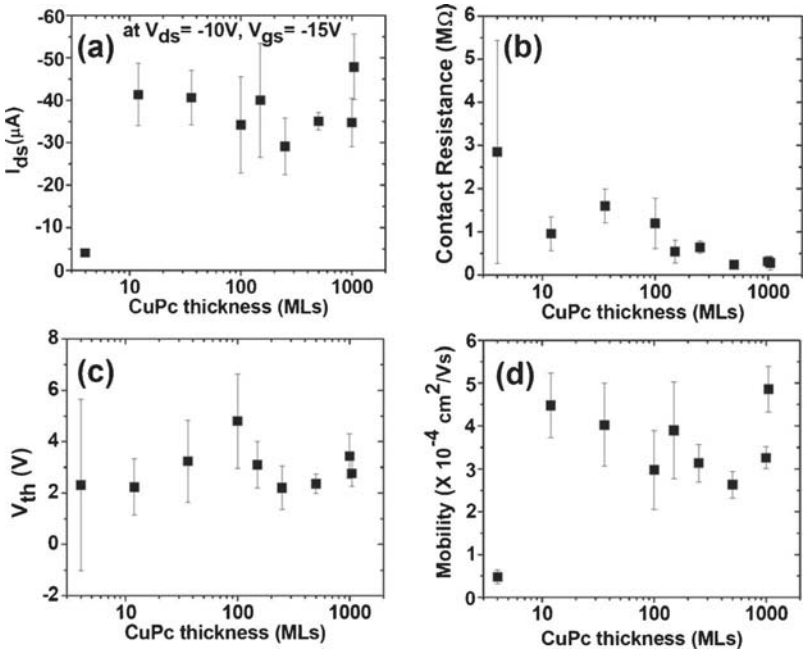

FIG. 7. (a) On-state current at $V_{ds}=-10$ V, $V_g=-15$ V, (b) contact resistance, (c) threshold voltage, and (d) mobility as a function channel thickness from CuPc OTFTs fabricated with the bilayer photoresist lift-off process.

also seen for the variations in the threshold voltages, as shown in Fig. 7(c). Though the rms roughness increased from 1.8 to 62 nm for the 12 and 1000 ML CuPc films, as shown in Fig. 4, the mobility and the threshold voltage were found to have only a small variation (less than 2 times) over 36 times change in film roughness and a 2.1 times change in island size. For all film thicknesses, the threshold voltage varies by less than 1 V (30%); this again is consistent with the density of grain boundaries playing a minimal role in the threshold voltage. Most importantly, the relatively narrow distributions of electrical properties in the bilayer lift-off processed devices are consistent with the control of the electrode profile in the first few nanometers above the surface.

IV. SUMMARY

The electrical properties of bottom contact CuPc OTFTs were investigated where the CuPc thickness varied over two orders of magnitude. The mobility and the threshold voltage were found to have only a small variation from 12 to 1000 ($\pm 5\%$) ML CuPc channel film thicknesses. The independence of measured electronic properties from channel thickness in this study is attributed to the contact resistance being negligible for all channel thicknesses with the use of tapered bottom contact electrodes.

ACKNOWLEDGMENTS

The authors thank the Calit2 Nano3 Nanofabrication Cleanroom Facility at UCSD. The USAFOSR is acknowledged for funding under MURI Grant No. F49620-02-1-0288 and NSF CHE-0350571.

[1] P. V. Necliudov, M. S. Shur, D. J. Gundlach, and T. N. Jackson, Solid-State Electron. **47**, 259 (2003).
[2] D. J. Gundlach, L. Zhou, J. A. Nichols, T. N. Jackson, P. V. Necliudov, and M. S. Shur, J. Appl. Phys. **100**, 024509 (2006).
[3] J. A. Nichols, D. J. Gundlach, and T. N. Jackson, Appl. Phys. Lett. **83**, 2366 (2003).
[4] L. Bürgi, T. J. Richards, R. H. Friend, and H. Sirringhaus, J. Appl. Phys. **94**, 6129 (2003).
[5] L. Torsi, F. Marinelli, M. D. Angione, A. Dell'Aquila, N. Cioffi, E. De Giglio, and L. Sabbatini, Org. Electron. **10**, 233 (2009).
[6] F. Dinelli, M. Murgia, P. Levy, M. Cavallini, F. Biscarini, and D. M. de Leeuw, Phys. Rev. Lett. **92**, 116802 (2004).
[7] T. Muck, V. Wagner, U. Bass, M. Leufgen, J. Geurts, and L. W. Molenkamp, Synth. Met. **146**, 317 (2004).
[8] J. Gao, J. B. Xu, M. Zhu, N. Ke, and D. Ma, J. Phys. D **40**, 5666 (2007).
[9] G. Horowitz, J. Mater. Res. **19**, 1946 (2004).
[10] J. Park, R. D. Yang, C. N. Colesniuc, A. Sharoni, S. Jin, I. K. Schuller, W. C. Trogler, and A. C. Kummel, Appl. Phys. Lett. **92**, 193311 (2008).
[11] C. W. Miller, A. Sharoni, G. Liu, C. N. Colesniuc, B. Fruhberger, and I. K. Schuller, Phys. Rev. B **72**, 104113 (2005).
[12] S. Luan and G. W. Neudeck, J. Appl. Phys. **72**, 766 (1992).
[13] V. Palermo, M. Palma, and P. Samorì, Adv. Mater. **18**, 145 (2006).
[14] K. P. Puntambekar, P. V. Pesavento, and C. D. Frisbie, Appl. Phys. Lett. **83**, 5539 (2003).
[15] Y. Hong, F. Yan, P. Migliorato, S. H. Han, and J. Jang, Thin Solid Films **515**, 4032 (2007).
[16] S. Cherian, C. Donley, D. Mathine, L. LaRussa, W. Xia, and N. Armstrong, J. Appl. Phys. **96**, 5638 (2004).
[17] L. Bürgi, H. Sirringhaus, and R. H. Friend, Appl. Phys. Lett. **80**, 2913 (2002).
[18] K. P. Gentry, T. Gredig, and I. K. Schuller, Phys. Rev. B **80**, 174118 (2009).
[19] D. K. Schroder, *Semiconductor Material and Device Characterization* (Wiley, New York, 1998).
[20] R. D. Yang, T. Gredig, C. N. Colesniuc, J. Park, I. K. Schuller, W. C. Trogler, and A. C. Kummel, Appl. Phys. Lett. **90**, 263506 (2007).